

An Axisymmetric Torsion Problem of an Elastic Layer on a Rigid Circular Base

B. Kebli^{1,*}, S. Berkane², F. Guerrache¹

¹Laboratoire de Génie Mécanique et Développement, Département de Génie Mécanique, Ecole Nationale Polytechnique El-Harrach Algiers 16200, Algeria

²Department of Computer Science and Engineering, University of Québec in Outaouais, Gatineau, Québec, Canada

Received 15 December 2019; accepted 20 February 2020

ABSTRACT

A solution is presented to a doubly mixed boundary value problem of the torsion of an elastic layer, partially resting on a rigid circular base by a circular rigid punch attached to its surface. This problem is reduced to a system of dual integral equations using the Boussinesq stress functions and the Hankel integral transforms. With the help of the Gegenbauer expansion formula of the Bessel function we get an infinite algebraic system of simultaneous equations for calculating the unknown function of the problem. Both the two contact stresses under the punch and on the lower face of the layer are expressed as appropriate Chebyshev series. The effects of the radius of the disc with the rigid base and the layer thickness on the displacements, contact stresses as well as the shear stress and the stress singularity factor are discussed. A numerical application is also considered with some concluding results. © 2020 IAU, Arak Branch. All rights reserved.

Keywords: Elastic torsion; Doubly mixed boundary value problem; Dual integral equations; Infinite algebraic system; Stress singularity factor.

1 INTRODUCTION

THE contact is the central problem of solids mechanics, because the contact zone is the main place where efforts are focused on a deformable body and represents the most critical point in the body. The mechanical contact is very important for the good resolution of many problems such as shaping (forging, stamping, punching, etc.) as well as for the simulation of wear (gears, tire-road, ...) and also for any system comprising several parts in a mechanical or multi-physical context. These problems are important for many industrial sectors, such as production, aeronautics, the automobile industry, railway and naval construction, civil engineering, the nuclear industry and the military. The theory of torsion of elastic bodies and methods for solving torsion problems present one of the vast areas of mathematical theory of elasticity. The theoretical and applied significance of contact torsion problems lies in the fact that they, on the one hand, generalize and develop the classical contact problems of the theory of elasticity. On the other hand, they are directly related to important practical engineering issues on the transfer of loads from thin-

*Corresponding author.
E-mail address: belkacem.kebli@g.enp.edu.dz (B. Kebli).

walled elements to massive deformable bodies, often encountered in construction, machine building, especially in aircraft building, in mechanics of growing bodies, in measurement technology, in composites mechanics, and in other fields of applied mechanics. The problem pertaining to the determination of the stresses and displacements in an elastic medium due to a torsional rotation of a rigid disc in bonded contact has been a subject of considerable interest in mechanics and applied mathematics. An explicit solution of the mixed boundary problem obtained by introducing in a suitable manner a system of oblate spheroidal coordinates for the static case of torsion deformation developed by Reissner and Sagocci [1]. Lebedev and Ufliand [2] treated the problem of pressing a stamp of circular cross-section into an elastic layer. They expressed the required displacements and stresses in terms of one auxiliary function, which represents the solution of a Fredholm integral equation with a continuous symmetrical kernel. Florence [3] interested of studied a solution analytics for the stress distribution at a rigid circular disk on an infinite elastic layer over a rigid foundation when the disk is subjected to either a torque about its axis or a moment about a diameter. The corresponding dual integral equations of the problem were solved using the Cooke's method. Strength of a composite elastic layer weakened by a plane circular crack, when a double elastic layer with a plane circular crack is subjected to torsion due to the rotation of a rigid cylindrical rod attached to the double layer is solved by Smelyanska [4]. The conjugation conditions ensure the stresses at the boundary separating the media and the displacements outside the crack. The shear stresses are give the corresponding systems of integral equations were reduced to a Fredholm integral equation of the second kind. Low [5] analyzed the effects of embedded flaws in an elastic half space subjected to torsional deformations. Specifically two types of flaws are considered: a penny-shaped rigid inclusion, and a penny-shaped crack. In each case the problem is reduced to a system of Fredholm integral equations. Graphical displays of the numerical results are included. The effect of an imperfectly bonded laminar composite is examined in terms of the intensification of the torsional stresses operative near the imperfection which is assumed to be a circular shaped area is considered by Sih and Chen [6] the laminar composite is modelled by four layers of different materials with the two outer layers being infinite in height and debonding occurs at the interface of the two inner layers. The analysis based on the application of Hankel transforms and the solution of a pair of dual integral equations can be easily extended to a multilayered system. Numerical results are obtained for two special laminate geometries and discussed with reference to the pertinent parameters used in the theory of fracture mechanics. The corresponding dual integral equations were reduced to a Fredholm one and solved numerically with the small parameter method. Torsion of elastic half-space with penny shaped crack is developed by Dhawan [7] the problem is reduced to a Fredholm integral equation. The effect of an embedded flaw in the form of a penny-shaped crack in an elastic half-space subjected to torsional oscillation was also studied. The torsion problem of two bonded layers by a rigid disc applied on it free surface was studied by Tamate [8]. A similar problem was examined by Singh and Dhaliwal [9]. The Reissner-Sagocci problem for an elastic layer under torsion by a pair of circular discs on opposite faces was considered. This problem is reduced to a pair of Fredholm integral equations which are then solved by the method of iteration. Gazetas [10] studied the effect of inhomogeneity on the axially symmetric elastic deformation arising in a soil deposit which is subjected to torsional shear tractions distributed linearly over a circular portion of the surface. Soil inhomogeneity is described by a shear modulus monotonically increasing with depth. The problem is formulated in terms of Hankel integral transforms. To obtain analytical expressions for displacement and stresses, in transform space, an inverse procedure has been devised in which the type of inhomogeneity has to be determined. As analytical inversion of the Hankel transforms of the resulting expression appears intractable, a simple numerical integration scheme is used to obtain the complete solution for stress and displacement distributions in the soil. An axisymmetric torsion problem of an elastic layer on a rigid foundation with a cylindrical hole treated by Hara et al. [11]. The problem is reduced to a solution of infinite systems of simultaneous equation. The obtained results are compared with the absence of the hole case. The problem with Torsion of two bonded layers by a rigid disc is developed by Erguven [12]. The elastostatic problem of torsion of a rigid disc bonded to a semi-infinite elastic solid at a finite depth considered by Pak and Saphores [13]. With the help of Hankel transforms, an exact formulation for the mixed boundary value problem is presented in the form of dual integral equations. They are, in turn, reduced to a Fredholm integral equation of the second kind, the solution of which is then computed. As illustrations, selected numerical results on the torque-rotation relationship, the stress and displacement fields, as well as the contact distribution are provided. Bacci [14] treated a rigid disk adheres perfectly to the upper surface of an elastic layer fixed to an undefonnable support. A rotation is applied to the disk around its axis. The resulting mixed boundary value problem is described by a Fredholm integral equation of the second kind. Under the assumption that the ratio of layer thickness to disk radius is not exceedingly small, an approximate explicit solution of this problem is given. Local stress field for torsion of penny-shaped crack in a functionally graded material considered by Li et al. [15]. Sakamoto [16] considered the axisymmetric problem on an elastic layer weakened by a circular crack subjected to an internal uniform pressure. The study considers the two cases when the surfaces of the layer are free of charge and smoothly clamped. These problems are reduced to dual integral equations

which are solved using an infinite system of algebraic equations by the Gegenbauer formula. The Reissner-Sagoci problem for a homogeneous coating on a functionally graded half-space is studied by Matysiak *et al.* [17]. The corresponding mixed boundary value problem was reduced to a Fredholm integral equation of the second kind and the authors used a quadrature method for its numerical solution. The problem of a penny-shaped crack problem in the interior of a homogeneous elastic material at the symmetry plane, under an axisymmetric torsion by two circular rigid discs symmetrically located in the elastic medium analyzed by Madani and Kebli [18]. The general solution of this problem is obtained by using the Hankel transforms method. The corresponding doubly mixed boundary value problem associated with the rigid disc and the penny-shaped is reduced to a system of dual integral equations, which are transformed, to a Fredholm integral equations of the second kind. Using the quadrature rule, the resulting system is converted to a system of infinite algebraic equations. Sakamoto [16] solved the same elastic layer weakened by a penny shaped as Lebedev [2] but using a different approach.

An analytical solution of an axisymmetric torsion problem of an elastic layer on a rigid circular base has been developed. We determine the solution of the elastic contact problem by the help Hankel integral transform method using the auxiliary Boussinesq stress functions. The doubly mixed boundary value problem is reduced to a system of dual integral equations. Instead of the classical Fredholm integral method the obtained solution is calculated from an infinite system of simultaneous algebraic equations by means of the Gegenbauer expansion formula of the Bessel function. The effects of the radius of the disc with the rigid base and the layer thickness on the displacements, stresses as well as the shear stress and the stress singularity factor are discussed. A numerical application is also considered with some concluding results. Our results are validated on the half space case and also on the problem dealt by Florence [3].

2 FORMULATION OF THE PROBLEM AND ITS SOLUTION

We use a cylindrical coordinate system (r, θ, z) . The Shear modulus of the elastic medium is noted by G . A general solution of this axisymmetric problem yields equilibrium equations that can be represented by Boussinesq's harmonic stress function φ_3 , where (u_r, v_θ, w_z) denotes the displacement vector and $(\sigma_r, \sigma_\theta, \sigma_z, \tau_{rz}, \tau_{\theta z}, \tau_{r\theta})$ the stress tensor, as follows:

$$\begin{cases} u_r = w_z = 0 \\ 2Gv_\theta = -\frac{\partial \varphi_3}{\partial r} \\ \tau_{\theta z} = -\frac{\partial^2 \varphi_3}{2\partial r \partial z} \\ \tau_{r\theta} = \frac{\partial^2 \varphi_3}{2\partial z^2} + \frac{\partial \varphi_3}{r \partial r} \\ \sigma_r = \sigma_\theta = \sigma_z = \tau_{rz} = 0 \end{cases} \quad (1)$$

The function φ_3 satisfy the following equation

$$\begin{cases} \nabla^2 \varphi_3 = 0 \\ \nabla^2 = \frac{\partial^2}{\partial r^2} + \frac{1}{r} \frac{\partial}{\partial r} + \frac{\partial^2}{\partial z^2} \end{cases} \quad (2)$$

We consider an isotropic elastic layer with thickness h , as shown in Fig. 1 which is a torsion around the vertical axis is applied to the surface of the layer by means of circular area of radius a by the disc with a plane base meanwhile about the z -axis through an angle ω_0 . The layer is resting on a rigid smooth circular base of radius b . The doubly mixed boundary value of the elastic layer can be described by the following equations on the rigid base

$$(v_\theta)_{z=0} = 0, \quad 0 \leq r \leq b \quad (3)$$

$$(\tau_{\theta z})_{z=0} = 0, \quad r > b \quad (4)$$

On the upper surface

$$(v_{\theta})_{z=h} = \omega_0 r, \quad 0 \leq r \leq a \tag{5}$$

$$(\tau_{\theta z})_{z=h} = 0, \quad r > a \tag{6}$$

All stress components vanish at infinity

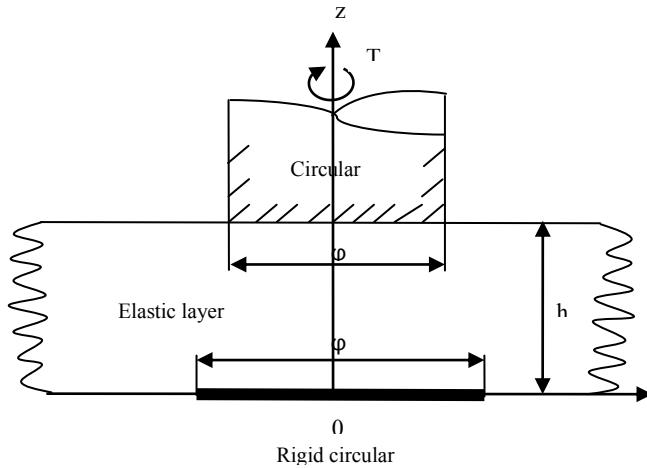


Fig.1
Geometry of the problem.

In order to satisfy the boundary condition (7), we can put the stress function φ_3 in this form

$$\varphi_3 = \int_0^{\infty} [A(\lambda) \sinh \lambda z + B(\lambda) \cosh \lambda z] J_0(\lambda r) d\lambda \tag{7}$$

where J_n is the Bessel function of the first kind in order n and $A(\lambda), B(\lambda)$ are unknown functions of λ . Using Eqs. (1) and (7), we obtain the components of displacements and stresses

$$2Gv_{\theta} = -\int_0^{\infty} \lambda [A(\lambda) \sinh \lambda z + B(\lambda) \cosh \lambda z] J_1(\lambda r) d\lambda \tag{8}$$

$$2\tau_{\theta z} = \int_0^{\infty} \lambda^2 [A(\lambda) \cosh \lambda z + B(\lambda) \sinh \lambda z] J_1(\lambda r) d\lambda \tag{9}$$

$$2\tau_{r\theta} = -\int_0^{\infty} \lambda^2 [A(\lambda) \sinh \lambda z + B(\lambda) \cosh \lambda z] J_2(\lambda r) d\lambda \tag{10}$$

A large contribution is made for solving the integral equation problem [19]. Using Eqs. (8), (9) and (10) the boundary conditions (4) to (5) lead to the following system of dual integral equations

$$2G(v_{\theta})_{z=h} = \int_0^{\infty} \lambda [A(\lambda) \sinh \lambda h + B(\lambda) \cosh \lambda h] J_1(\lambda r) d\lambda = 2G\omega_0 r, \quad 0 \leq r \leq a \tag{11}$$

$$2G(v_{\theta})_{z=0} = \int_0^{\infty} \lambda B(\lambda) J_1(\lambda r) d\lambda = 0, \quad 0 \leq r \leq b \tag{12}$$

$$2(\tau_{\theta z})_{z=h} = \int_0^{\infty} \lambda^2 [A(\lambda) \cosh \lambda h + B(\lambda) \sinh \lambda h] J_1(\lambda r) d\lambda = 0, \quad r > a \quad (13)$$

$$2(\tau_{\theta z})_{z=0} = \int_0^{\infty} \lambda^2 A(\lambda) J_1(\lambda r) d\lambda = 0, \quad r > b \quad (14)$$

Making use of the following integral formula [20]

$$\int_0^{\infty} \lambda J_1(\lambda r) M_n(\lambda x) d\lambda = \begin{cases} \frac{2 T_{2n+1}(r/x)}{\pi \sqrt{x^2 - r^2}}, & r < x \\ 0, & r > x \end{cases} \quad (15)$$

where T_{2n+1} is the Tchebycheff function of the first kind and

$$M_n(\lambda x) = \frac{\partial}{\partial \lambda} \left[J_{\left(n+\frac{1}{2}\right)}(\lambda x/2) J_{-\left(n+\frac{1}{2}\right)}(\lambda x/2) \right] \quad (16)$$

and

$$\int_0^{\infty} J_1(\lambda r) \sin \lambda x d\lambda = \begin{cases} \frac{x}{r \sqrt{r^2 - x^2}}, & x < r \\ 0, & x > r \end{cases} \quad (17)$$

In order to satisfy the homogeneous Eqs. (13) and (14), we can set

$$\begin{cases} \lambda \omega_* [A(\lambda) \cosh \lambda h + B(\lambda) \sinh \lambda h] = \sum_{n=0}^{\infty} \alpha_n M_n(\lambda a) \\ \lambda \omega_* A(\lambda) = \sum_{n=0}^{\infty} \beta_n M_n(\lambda b) \end{cases} \quad (18)$$

where

$$\omega_* = -\frac{1}{G \omega_0 a^2} \quad (19)$$

Solving this system of two equations yields the determination of the function $B(\lambda)$

$$\lambda \omega_* B(\lambda) = \sum_{n=0}^{\infty} \left[\alpha_n \frac{1}{\sinh \lambda h} M_n(\lambda a) - \beta_n \coth \lambda h M_n(\lambda b) \right] \quad (20)$$

Now if we substitute Eq. (20) into the Eqs. (11) and (12), we get

$$\sum_{n=0}^{\infty} \int_0^{\infty} \left[\alpha_n \coth \lambda h M_n(\lambda a) - \beta_n \frac{1}{\sinh \lambda h} M_n(\lambda b) \right] J_1(\lambda r) d\lambda = -\frac{2r}{a^2}, \quad 0 \leq r \leq a \quad (21)$$

$$\sum_{n=0}^{\infty} \int_0^{\infty} \left[\alpha_n \frac{1}{\sinh \lambda h} M_n(\lambda a) - \beta_n \coth \lambda h M_n(\lambda b) \right] J_1(\lambda r) d\lambda = 0, \quad 0 \leq r \leq b \quad (22)$$

Making use the following Gegenbauer's formula [20]

$$-rJ_1(\lambda r) = \sum_{m=0}^{\infty} (2 - \delta_{0m}) X_m(\lambda x) \cos 2m\phi_x, \quad (\phi_x = \sin^{-1}(r/x) \text{ and } 0 \leq r \leq x; x = a, b) \tag{23}$$

where

$$X_m(\lambda x) = \partial J_m^2\left(\frac{\lambda x}{2}\right) / \partial \lambda, \quad (x = a, b \text{ and } m = 0, 1, \dots) \tag{24}$$

and δ_{0m} denotes the Kronecker delta, $\delta_{nm} = \begin{cases} 1, & m = n \\ 0, & m \neq n \end{cases}$

Using the formula (23) into the Eqs. (21) and (22), we obtain

$$\sum_{n=0}^{\infty} \int_0^{\infty} \left[\alpha_n \coth \lambda h M_n(\lambda a) - \beta_n \frac{1}{\sinh \lambda h} M_n(\lambda b) \right] \sum_{m=0}^{\infty} (2 - \delta_{0m}) X_m(\lambda a) \cos 2m\phi_a d\lambda = 1 - \cos 2\phi_a \tag{25}$$

$$\sum_{n=0}^{\infty} \int_0^{\infty} \left[\alpha_n \frac{1}{\sinh \lambda h} M_n(\lambda a) - \beta_n \coth \lambda h M_n(\lambda b) \right] \sum_{m=0}^{\infty} (2 - \delta_{0m}) X_m(\lambda b) \cos 2m\phi_b d\lambda = 0 \tag{26}$$

Matching the coefficients of $\cos 2m\phi_{a,b}$ on both sides of Eqs. (25) and (26), we obtain the following infinite system of simultaneous equations for the determination of α_n and β_n

$$\begin{cases} \sum_{n=0}^{\infty} \int_0^{\infty} \left[\alpha_n \coth \lambda h M_n(\lambda a) - \beta_n \frac{1}{\sinh \lambda h} M_n(\lambda b) \right] X_m(\lambda a) d\lambda = \delta_{0m} - \delta_{1m} / 2 \\ \sum_{n=0}^{\infty} \int_0^{\infty} \left[\alpha_n \frac{1}{\sinh \lambda h} M_n(\lambda a) - \beta_n \coth \lambda h M_n(\lambda b) \right] X_m(\lambda b) d\lambda = 0 \end{cases} \tag{27}$$

In matrix form the last system can be writing as:

$$\begin{cases} \sum_{n=0}^{\infty} [\alpha_n A_{nm} - \beta_n B_{nm}] = \delta_{0m} - \delta_{1m} / 2 \\ \sum_{n=0}^{\infty} [\alpha_n C_{nm} - \beta_n D_{nm}] = 0 \end{cases} \tag{28}$$

where

$$\begin{aligned} A_{nm} &= \int_0^{\infty} \coth \lambda h M_n(\lambda a) X_m(\lambda a) d\lambda \\ B_{nm} &= \int_0^{\infty} \frac{1}{\sinh \lambda h} M_n(\lambda b) X_m(\lambda a) d\lambda \\ C_{nm} &= \int_0^{\infty} \frac{1}{\sinh \lambda h} M_n(\lambda a) X_m(\lambda b) d\lambda \\ D_{nm} &= \int_0^{\infty} \coth \lambda h M_n(\lambda b) X_m(\lambda b) d\lambda \end{aligned} \tag{29}$$

2.1 Displacements and stresses on two layer boundaries

The components of displacement on both the upper and lower surfaces of the layer can be expressed as follows:

$$(v_{\theta}^*)_{z=0} = \frac{(v_{\theta})_{z=0}}{a\omega_0} = -\frac{a}{2}H(r-b) \sum_{n=0}^{\infty} \int_0^{\infty} \left[\alpha_n M_n(\lambda a) \frac{1}{\sinh \lambda h} - \beta_n M_n(\lambda b) \coth \lambda h \right] J_1(\lambda r) d\lambda \quad (30)$$

$$(v_{\theta}^*)_{z=h} = \frac{(v_{\theta})_{z=h}}{a\omega_0} = \frac{r}{a}H(a-r) - \frac{a}{2}H(r-a) \sum_{n=0}^{\infty} \int_0^{\infty} \left[\alpha_n M_n(\lambda a) \coth \lambda h - \beta_n M_n(\lambda b) \frac{1}{\sinh \lambda h} \right] J_1(\lambda r) d\lambda \quad (31)$$

where H denotes Heaviside unit step function from Eqs. (30) and (31), we find that $H(x-r) = \begin{cases} 1, & r < x \\ 0, & r > x \end{cases}$

We can deduce that shears stresses, on both the upper and the lower surfaces of the layer, are expressed as appropriate Chebyshev series, as follows:

$$(\tau_{\theta z}^*)_{z=0} = \omega_* (\tau_{\theta z})_{z=0} = -\frac{1}{\pi}H(b-r) \sum_{n=0}^{\infty} \beta_n \frac{T_{2n+1}(r/b)}{\sqrt{b^2-r^2}} \quad (32)$$

$$(\tau_{\theta z}^*)_{z=h} = \omega_* (\tau_{\theta z})_{z=h} = -\frac{1}{\pi}H(a-r) \sum_{n=0}^{\infty} \alpha_n \frac{T_{2n+1}(r/a)}{\sqrt{a^2-r^2}} \quad (33)$$

The torque T to indent the disc is given by

$$T = -2\pi \int_0^a (\tau_{\theta z})_{z=h} r^2 dr = 4G\omega_0 a^4 \sum_{n=0}^{\infty} \frac{(-1)^{n+1} \alpha_n}{(2n-1)(2n+1)(2n+3)} \quad (34)$$

The stress singularity factors corresponding to the studied problem are defined by

$$S_0 = \lim_{r \rightarrow b^-} \sqrt{2\pi(r-b)} \frac{(\tau_{\theta z})_{z=0}}{G\omega_0} \quad (35)$$

$$S_h = \lim_{r \rightarrow a^-} \sqrt{2\pi(r-a)} \frac{(\tau_{\theta z})_{z=h}}{G\omega_0} \quad (36)$$

Substituting Eqs. (32), (33) into Eqs. (35) and (36), we obtain the simple expression for the stress singularity factors as following

$$S_0 = \frac{b}{\sqrt{\pi}} \sum_{n=0}^{\infty} \beta_n \quad (37)$$

$$S_h = \frac{a}{\sqrt{\pi}} \sum_{n=0}^{\infty} \alpha_n \quad (38)$$

3 VALIDATION OF THE RESULTS

3.1 With the case of half space

As a particular case, we can find that for $b = 0$ and $h \rightarrow \infty$, the infinite integrals of the system (28) leads to

$$\sum_{n=0}^{\infty} \alpha_n \int_0^{\infty} M_n(\lambda a) X_m(\lambda a) d\lambda = \delta_{0m} - \delta_{1m} / 2 \quad (m=0, 1, \dots) \tag{39}$$

From Eq. (39) we can get $\alpha_0 = \frac{4}{a}, \alpha_n = 0, (n \geq 1)$. In addition, the expressions for surface displacement, contact stress and the torque are given by

$$\begin{aligned} \frac{(v_{\theta})_{z=h}}{a\omega_0} &= \frac{r}{a} - \frac{2}{\pi} H(r-a) \left[\frac{r}{a} \cos^{-1} \frac{r}{a} + \frac{\sqrt{r^2 - a^2}}{r} \right] \\ \frac{(\tau_{\theta z})_{z=h}}{G\omega_0} &= \frac{4r}{\pi\sqrt{a^2 - r^2}} H(a-r) \\ \frac{(\tau_{r\theta})_{z=h}}{G\omega_0} &= -\frac{4a^3}{\pi r^2 \sqrt{r^2 - a^2}} H(r-a) \end{aligned} \tag{40}$$

and $\frac{T}{G\omega_0 a^3} = \frac{16}{3}$

Eqs. (40) are those of the torsion of an elastic half-space by a circular rigid punch

3.2 With the problem of FLORANCE [3]

The problem dealt with by Florence [3] is a particular case of our study and can be recovered in the case where the radius of the rigid base b is stretched towards infinity

4 NUMERICAL RESULTS AND DISCUSSIONS

To determine the unknown coefficients α_n and β_n discussed in previous section, we must evaluate the infinite integrals of the system (28). By separating into the terms obtained by numerical integration and those by an application of the asymptotic expansions of Bessel functions. It is clear that for large values of λ we get $\coth \lambda h \rightarrow 1$ and $\frac{1}{\sinh \lambda h} \rightarrow 0$. This allows us to write

$$\begin{aligned} A_{nm} &\approx \int_0^{\lambda_0} \coth \lambda h M_n(\lambda a) X_m(\lambda a) d\lambda + \int_{\lambda_0}^{\infty} M_n(\lambda a) X_m(\lambda a) d\lambda \\ B_{nm} &\approx \int_0^{\lambda_0} \frac{1}{\sinh \lambda h} M_n(\lambda b) X_m(\lambda a) d\lambda \\ C_{nm} &\approx \int_0^{\lambda_0} \frac{1}{\sinh \lambda h} M_n(\lambda a) X_m(\lambda b) d\lambda \\ D_{nm} &\approx \int_0^{\lambda_0} \coth \lambda h M_n(\lambda b) X_m(\lambda b) d\lambda + \int_{\lambda_0}^{\infty} M_n(\lambda b) X_m(\lambda b) d\lambda \end{aligned} \tag{41}$$

The first integrals of the right landside of the above expressions are evaluated numerically using the Simpson formula. Here, we choose 1000 subintervals and $\lambda_0 = 1500$ and the second one is replaced by the integral of the

function equivalent. Next we evaluate asymptotically the integral term $\int_{\lambda_0}^{\infty} M_n(\lambda x) X(\lambda x) d\lambda$. As for large value of λ we have

$$J_\nu(\lambda x) \approx \sqrt{\frac{2}{\pi \lambda x}} \left[\cos\left(\lambda x - \frac{\pi}{2}\nu - \frac{\pi}{4}\right) - \frac{4\nu^2 - 1}{8\lambda x} \sin\left(\lambda x - \frac{\pi}{2}\nu - \frac{\pi}{4}\right) + o\left(\frac{1}{(\lambda x)^2}\right) \right] \lambda x \rightarrow +\infty \quad (42)$$

$$J_{\left(n+\frac{1}{2}\right)}\left(\frac{\lambda x}{2}\right) J_{-\left(n+\frac{1}{2}\right)}\left(\frac{\lambda x}{2}\right) \approx 4\left(\frac{1}{2}+n\right)^2 \frac{\cos \lambda x}{\pi(\lambda x)^2} \quad (43)$$

whereas

$$M_n(\lambda x) \approx -\frac{8(1+n)}{\pi(\lambda x)^2} \cos \lambda x \quad (44)$$

Then $M_n(\lambda x) X_m(\lambda x)$ is replaced by for large values of λ

$$\frac{4}{\pi^2(\lambda x)^2} \left[\sin \lambda x + \frac{(-1)^m}{2}(1 - \cos(2\lambda x)) \right] \quad (45)$$

and of the relation obtained by integration par parts

$$\int_{\lambda_0}^{\infty} \frac{\cos^2 \lambda x}{(\lambda x)^2} d\lambda = \frac{\cos^2 \lambda_0 x}{\lambda_0 x} + x \operatorname{si}(2\lambda_0 x) \quad (46)$$

Then

$$\int_{\lambda_0}^{\infty} M_n(\lambda x) X_n(\lambda x) d\lambda \approx \frac{4}{\pi^2(x)^2} \left\{ \frac{\sin \lambda_0 x}{\lambda_0} - x \operatorname{ci} \lambda_0 x + \frac{(-1)^m}{2} \left[\frac{1 - \cos(2\lambda_0 x)}{\lambda_0} - 2x \operatorname{si}(2\lambda_0 x) \right] \right\} \quad (47)$$

where $\operatorname{si}(x)$ is the integral sine function

$$\operatorname{si}(x) = -\int_x^{\infty} \frac{\sin \xi}{\xi} d\xi \quad (48)$$

and $\operatorname{ci}(x)$ is the integral cosine function

$$\operatorname{ci}(x) = -\int_x^{\infty} \frac{\cos \xi}{\xi} d\xi \quad (49)$$

The coefficients elastics α_n and β_n are shown in the following Tables 1-4., of the thickness elastic layer and the radius of the disc with the rigid base

Table 1

Values of the coefficients elastics α_n and β_n for $h/a=1$ and various values of b/a .

n	$b/a=0.5$	$b/a=1$	$b/a=1.5$
α_n			
0	3.739611017953796	3.983788899757462	4.172067903177652
1	0.007953367469361	-0.056260500481093	-0.055859698704046
2	0.006142138541829	0.007944861070421	0.003277751091580
3	-0.001383963487921	-0.000057591486065	0.000057176309999
4	0.000086926681302	-0.000182303527505	-0.000129000315475
5	0.000111526581392	0.000140535686355	0.000143549111475
6	-0.000156306134004	-0.000165570916663	-0.000173991179636
7	0.000137662682455	0.000146411921175	0.000153399746710
8	-0.000208501521969	-0.000221320067071	-0.000231754455384
9	0.000109065714806	0.000117192869601	0.000122745667823
β_n			
0	0.694558542611535	1.128889430215339	1.189557456551056
1	-0.048356555962049	-0.338727521884290	-0.817546523415613
2	0.000719945930218	0.029664248400491	0.204180579779440
3	0.000016562704126	0.000678220790190	-0.017851315642931
4	-0.000000851174826	-0.000363002573279	-0.004381568529923
5	-0.000008264945399	0.000050187962416	0.001649822836933
6	-0.000011700614137	-0.000043196952790	-0.000127730381337
7	-0.000032522537498	0.000042790425714	-0.000057990711221
8	-0.000052623746738	-0.000059836672665	0.000020435943586
9	-0.000101577590032	0.000038558000572	-0.000009672824829

Table 2

Values of the coefficients elastics α_n and β_n for $b/a=1$ and various values of h/a .

n	$h/a=0.7$	$h/a=1$	$h/a=1.5$
α_n			
0	4.170033382782129	3.983788899757462	3.950183204524812
1	-0.212832588510739	-0.056260500481093	-0.006590598710702
2	0.025738241321176	0.007944861070421	0.000969978084557
3	0.001702889430108	-0.000057591486065	0.000049411164114
4	-0.000452062863889	-0.000182303527505	-0.000126213922232
5	0.000091219012651	0.000140535686355	0.000136362204521
6	-0.000166391798562	-0.000165570916663	-0.000164807531420
7	0.000155482765676	0.000146411921175	0.000144990450539
8	-0.000230395062599	-0.000221320067071	-0.000219844561831
9	0.000124966919117	0.000117192869601	0.000115403489395
β_n			
0	1.895863774517311	1.128889430215339	0.541813542818172
1	-0.684440732310698	-0.338727521884290	-0.115525955216694
2	0.040394254408903	0.029664248400491	0.009707885327886
3	0.009627421603626	0.000678220790190	-0.000367394955728
4	-0.000888507158191	-0.000363002573279	-0.000025305369857
5	-0.000158078097548	0.000050187962416	0.000020876338087
6	-0.000056572072881	-0.000043196952790	-0.000022513856425
7	0.000078093408042	0.000042790425714	0.000020496765178
8	-0.000099187351701	-0.000059836672665	-0.000029139819080
9	0.000066021665867	0.000038558000572	0.000017757790383

Table 3Values of the coefficients elastics α_n and β_n for $b = 0$ and $h/a \rightarrow \infty$.

n	α_n
0	3.999997992791846
1	0.000061598423155
2	-0.000087455362930
3	0.000108167777386
4	-0.000128018135665
5	0.000137877319537
6	-0.000166881799914
7	0.000146782730313
8	-0.000222671264024
9	0.000116752007792
n	$\beta_n (10^{-6})$
0	0.350287408318305
1	-0.000006503405484
2	0.000089393103665
3	-0.000061046583542
4	-0.000003876527967
5	-0.000470600174289
6	-0.000806790373148
7	-0.002083069207280
8	-0.003500326973150
9	-0.006398628018515

Table 4Values of the coefficients elastics α_n and β_n for $h/a=2$ and $b/a \rightarrow \infty$.

n	α_n
0	3.943638872732461
1	0.002694533965913
2	-0.000152751183762
3	0.000107950815758
4	-0.000126236171898
5	0.000135931710572
6	-0.000164535666511
7	0.000144700338121
8	-0.000219558348177
9	0.000115060148000
n	$\beta_n (10^{-6})$
0	0.005456878103825
1	-0.014846961065098
2	0.029711734090734
3	-0.031573804154084
4	0.056723557241741
5	-0.046962754343598
6	0.082742719325882
7	-0.067199019594041
8	0.096912234170243
9	-0.115520253799589

The distribution of the nondimensional normal displacements and shear stress with different values of plan z/h is graphically illustrated in the Figs. 2 and 3.

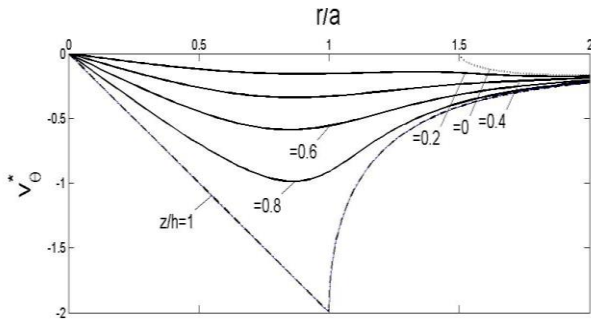


Fig.2
The variation of v_{θ}^* for $b/a=1.5$ with various values of z/h .

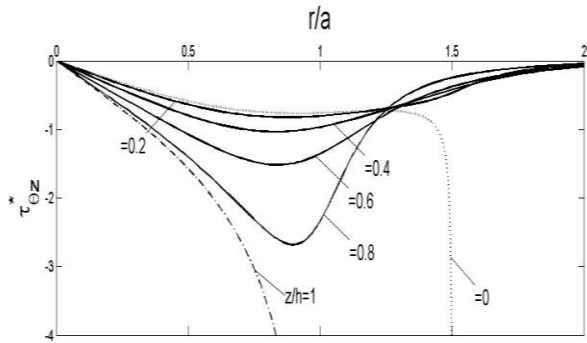


Fig.3
The variation of $\tau_{\theta z}^*$ for $b/a=1.5$ with various values of z/h .

Figs. 4 and 5 show the variation of the nondimensional normal displacement $(v_{\theta}^*)_{z=0}$ for h/a and b/a , respectively. It decreases with decreasing the layer thickness and the radius of the rigid base

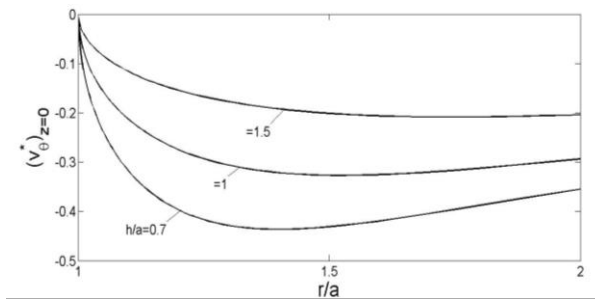


Fig.4
The variation of $(v_{\theta}^*)_{z=0}$ for $b/a=1.5$ and various values of h/a .

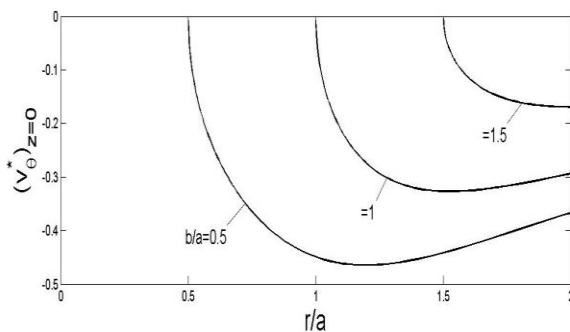


Fig.5
The variation of $(v_{\theta}^*)_{z=0}$ for $h/a=1.5$ and various values of b/a .

The distribution of the nondimensional shear stress $(\tau_{\theta z}^*)_{z=0}$ at the rigid base is given in Fig. 6 with various values of h/a . It is noted that the value are decreasing with decreasing the layer thickness. The values of the nondimensional shear stress decreasing the rigid base radius are illustrated in Fig. 7.

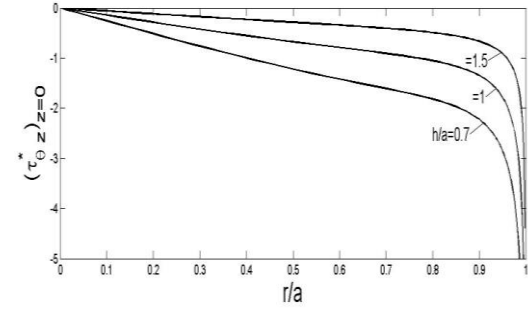


Fig.6
The variation of $(\tau_{\theta z}^*)_{z=0}$ for $b/a=1.5$ and various values of h/a .

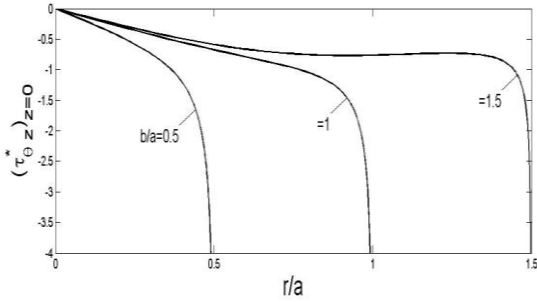


Fig.7
The variation of $(\tau_{\theta z}^*)_{z=0}$ for $h/a=1.5$ and various values of b/a .

The variations of the torque T^* applied to the disc with the layer thickness and rigid base are mentioned in Figs. 8 and 9. The horizontal line represents the case when $h/a \rightarrow \infty$ (an elastic half-space). When the value of T^* change with the layer thickness and the rigid base radius. From the graph line in the Fig.10, it shows a good agreement with those obtained by Florence [3] or the torque T^* decreases with increasing the layer thickness.

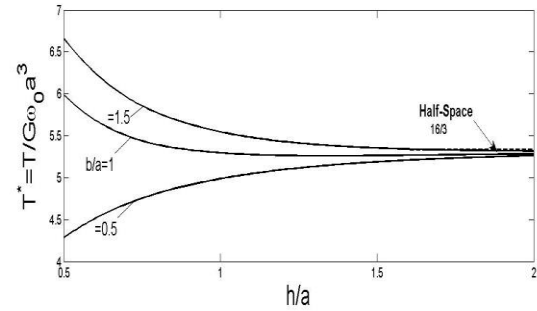


Fig.8
The variation of T^* for various values of h/a .

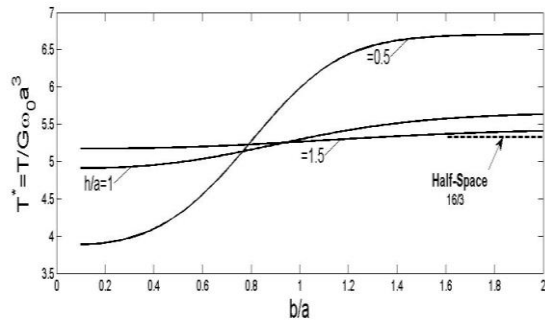


Fig.9
The variation of T^* for various values of b/a .

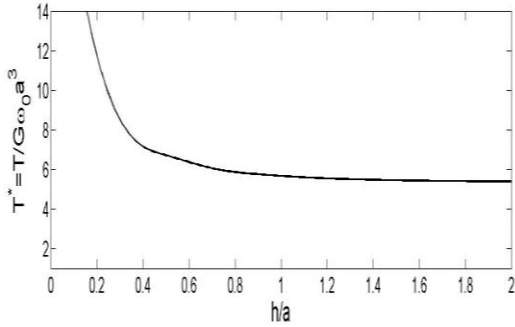


Fig.10
The variation of T^* for $b/a \rightarrow \infty$ and various values of h/a .

The variation of the stress singularity factors corresponding to the studied problem is graphically illustrated in Figs. 11 and 12. It is clear that the effect of the layer thickness and the rigid base radius in the distribution of the stress singularity factors S_0, S_h

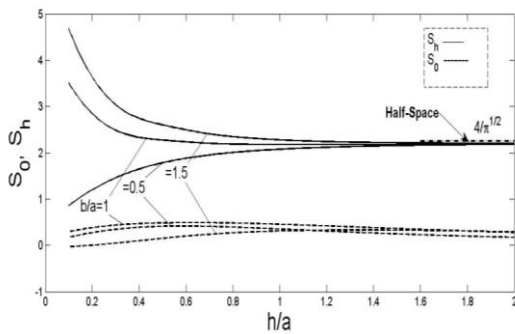


Fig.11
The variation of S_0, S_h for various values of h/a .

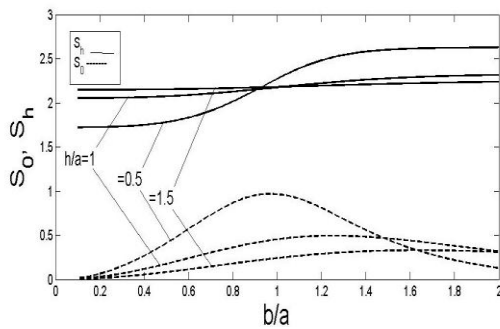


Fig.12
The variation of S_0, S_h for various values and b/a .

5 CONCLUSIONS

In the present paper, we studied a doubly mixed boundary value problem for an elastic layer. An analytical solution was obtained for the corresponding dual integral equations system through an infinite system of simultaneous equations using the Gegenbauer formula.

The obtained results are summarized as follows:

- Analytical solution based upon the integral Hankel transforms for contact problem have been developed and utilized.
- By the truncation method. An infinite algebraic system has been solved with different values of the elastic layer thickness and the radius of the disc with the rigid base.
- The numerical results revealed the effects of the layer thickness and the radius of the disc with the rigid base on the displacement, the torque as well as on the stress singularity factors.

The graphs obtained are analyzed as follows:

- The distribution of the nondimensional normal displacements and shear stress with different values of plan z/a is graphically presented.
- The distribution of the nondimensional normal displacements $(v_{\theta}^*)_{z=0}$ decreases with decreasing the layer thickness and the radius of the rigid base.
- The distribution of the nondimensional shear stresses $(\tau_{\theta z}^*)_{z=0}$ at the rigid base is given with various values of h/a . It is noted that the value are decreasing with decreasing the layer thickness and the rigid base radius, graphically they are displayed.
- The variations of the torque T^* applied to the disc and the stress singularity factors S_0, S_h with the layer thickness and rigid base are mentioned graphically. It is noted that the value of T^* and S_0, S_h change with the layer thickness and the rigid base radius.
- The graphical results illustrated effects of the radius of the disc with the rigid base and the layer thickness on the displacements, stresses as well as the shear stress and the stress singularity factors.
- The results are validated on the half space case and it shows a good agreement with those obtained by Florence [3] when the radius of the rigid base b is stretched towards infinity.

REFERENCES

- [1] Reissner E., Sagoci H.F., 1944, Forced torsion oscillation of a half-space-I, *Journal of Applied Physics* **15**: 652-654.
- [2] Lebedev N.N., Ufliand I.S., 1958, Axisymmetric contact problem for an elastic layer, *PMM* **22**: 320-326.
- [3] Florence A.L., 1961, Two contact problems for an elastic layer, *The Quarterly Journal of Mechanics and Applied Mathematics* **14**: 453-459.
- [4] Smelyanskaya L.M., Tokar A.S., 1971, Strength of a composite elastic layer weakened by a plane circular crack, *Soviet Applied Mechanics* **7**: 1119-1125.
- [5] Low R.D., 1972, On the torsion of elastic half spaces with embedded penny shaped flaws, *Journal of Applied Mechanics* **72**: 786-790.
- [6] Sih G.C., Chen E.P., 1972, Torsion of a laminar composite de bonded over a penny- shaped area, *Journal of the Franklin Institute* **293**: 251-261.
- [7] Dhawan G.K., 1974, Torsion of elastic half-space with penny shaped crack, *Defence Science Journal* **24**: 15-22.
- [8] Tamate O., Saito T., 1975, On the twisting of two elastic layers bonded to a rigid foundation, *Translations of the Japan Society of Mechanical Engineers* **341**: 33-40.
- [9] Singh B.M., Dhaliwal R.S., 1977, Torsion of an elastic layer by two circular dies, *International Journal of Engineering Science* **15**: 171-175.
- [10] Gazetas G., 1981, Torsional displacements and stresses in non-homogeneous soil, *Geotechnique* **31**: 487-496.
- [11] Hara T., Akiyama T., Shibuya T., Koizumi T., 1989, An axisymmetric torsion problem of an elastic layer on a rigid foundation with a cylindrical hole, *Translations of the Japan Society of Mechanical Engineers* **55**: 1339-1346 .
- [12] Erguven M.E., 1991, Torsion of two bonded layers by a rigid disc, *Meccanica* **26**: 117-123.
- [13] Pak R.Y.S., Saphores J.D.M., 1991, Torsion of a rigid disc in a half-space, *International Journal of Engineering Science* **29**: 1-12 .
- [14] Bacci A., Bennati S., 1996, An approximate explicit solution for the local torsion of an elastic layer, *Mechanics of Structures and Machines* **24**: 21-38.
- [15] Li C., Zou Z., 1998, Local stress field for torsion of penny-shaped crack in a functionally graded material, *International Journal of Fracture* **91**: 17-22.
- [16] Sakamoto M., 2003, An elastic layer with a penny-shaped crack subjected to internal pressure, *SME International Journal Series A solid Mechanics and Material Engineering* **46**: 10-14.
- [17] Matysiak S.J., Kulchytsky-Zhyhailo R., Perkowski D.M., 2011, Reissner-Sagoci problem for a homogeneous coating on a functionally graded half-space, *Mechanics Research Communications* **38**: 320-325.
- [18] Madani F., Kebli B., 2017, Axisymmetric torsion of an internally cracked elastic medium by two embedded rigid discs, *Mechanics and Mechanical Engineering* **21**: 363-377.
- [19] Duffy D.G., 2008, *Mixed Boundary Value Problems*, Boca Raton, Chapman Hall/CRC.
- [20] Gradshteyn I.S., Ryzhik I.M., 2007, *Table of Integrals- Series and Products*, Academic Press, New York.